Supplementary materials to "Digesting fossil infrastructure for cleaner energy transitions"

Hauke Schlesier[1,2], Gonzalo Guillén-Gosálbez*[2], Harald Desing*[1]

[1] Technology and Society Laboratory, Empa – Swiss Federal Laboratories for Materials Science and Technology, St. Gallen, Switzerland
[2] Institute for Chemical and Bioengineering, Department of Chemistry and Applied Biosciences, ETH Zürich, Zürich, Switzerland.
* corresponding author:
gonzalo.guillen.gosalbez@chem.ethz.ch
harald.desing@empa.ch

Contents

S1 Mitigation pathways and temperature trajectories of scenarios 2

S2 Annual production of materials 2

S3 Steel production cost 3

S4 Capacity potential of steel 3

S5 Steel use in photovoltaic systems 3

S6 Carbon footprints of green hydrogen and methanol 4

S7 Value of steel scrap in fossil infrastructure 5

S8 Limitations and robustness of results 5

S9 Material intensities of fossil infrastructure and their uncertainty 6
S9.1 Material intensities 6
S9.2 Uncertainties 6

S10 Steel life cycle assessment 8
S10.1 Goal, scope, and system boundaries 8
S10.2 Scrap transport estimation 10
S10.3 Steel production efficiencies 10
S10.4 Inventory adjustments for electric arc furnace hexavalent chromium content in slag and dust 11

S11 Life cycle impact indicators 12

The content in the supplementary material appears in the same order as it is referred to in the main manuscript.

S1 Mitigation pathways and temperature trajectories of scenarios

In this study, we investigate three Shared Socioeconomic Pathways (SSPs)—SSP1 (Sustainability), SSP2 (Middle-of-the-road), and SSP5 (Fossil-fueled development)—, which are the SSPs available in Premise v2.2.3 [1]. We further investigate two variations: Nationally Determined Contributions (NDC), which are domestic climate mitigation efforts each party to the Paris Agreement has to prepare and communicate in order to fulfill the collective target [2], and National Policies implemented (NPi), which are climate policies currently implemented.

Figure S1 (left) shows the climate mitigation pathways according to investigated scenarios. Transition times are 70 years or longer and even more than 25 years in very ambitious scenarios (SSP1-PkBudg900; cumulative carbon budget does not exceed 900 Gt CO_2). The time required to recycle steel in current fossil infrastructure (five to 14 years with continental steel waste trade) with idle capacity is therefore well within time periods of typical transitions. Recycling can thus contribute to steel supply in the transition.

Figure S1 (right) shows global mean temperature trajectories. Scenarios such as SSP1-NPi, SSP2-NDC, and SSP1-NPi lead to global warming similar to what is expected today (2.5 to 2.9 °C) [3] (see Fig. S1, right panel).

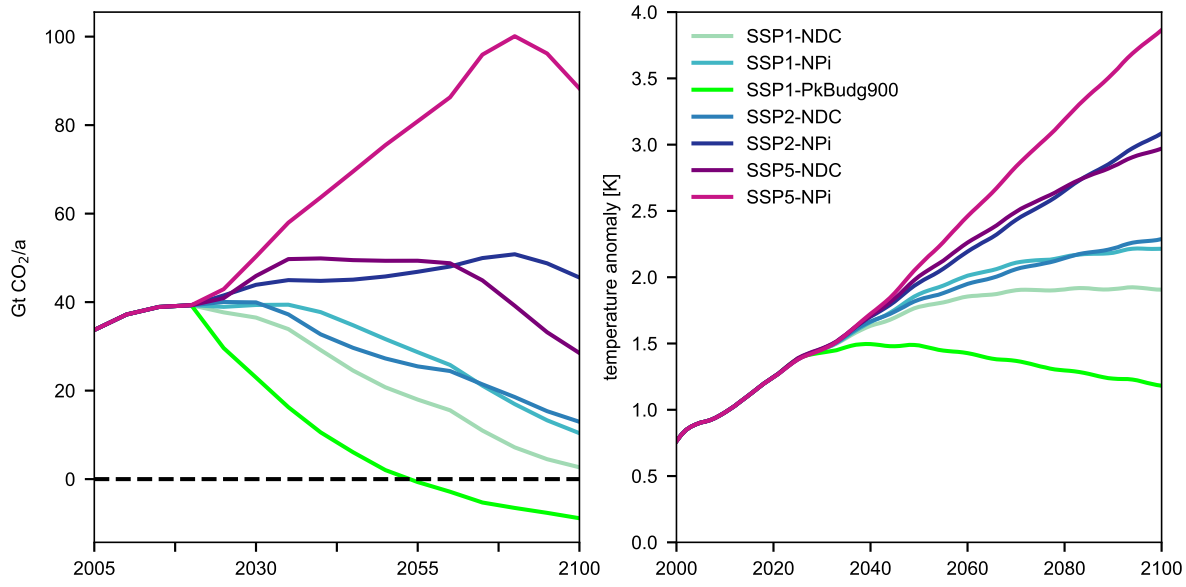

Figure S1: **Carbon dioxide mitigation pathways and temperature trajectories.** Carbon dioxide mitigation pathways of investigated scenarios and SSP1-PkBudg900 in the left panel. All investigated pathways have a transition time of multiple decades, even very ambitious scenarios (SSP1-PkBudg900) have a transition time of around 30 years. Projected temperature increases compared to pre-industrial scenarios until 2100 are shown in the right panel. End-of-century temperature increases of investigated scenarios range from 1.9 °C to 3.9 °C.

S2 Annual production of materials

In Figure 2 of the main manuscript, we show annual production data for several materials. The production values, year of production, and data source are shown in Table S1.

Table S1: Global annual production of materials shown in Figure 2 (main manuscript).

Material	**Total Production [Mt]**	**Year**	**Source**
Concrete	3.00×10^{3}	2017	[4]
Sand	5.00×10^{4}	2022	[5]
Steel	1.90×10^{3}	2023	[6]
Wood	1.07×10^{3}*	2023	[7]
Act. bentonite	1.80×10^{1}	2021	[8]
Barite	8.50×10^{0}	2023	[9]
PE	1.05×10^{2}	2022	[10]
Cu	2.70×10^{1}	2023	[11]
Stone wool	1.00×10^{1}**	2021	[12]
Al	6.80×10^{1}	2021	[13]
Rubber	3.00×10^{1}	2022	[14]
Fe	1.30×10^{3}	2023	[6]
Lignite	6.39×10^{2}	2020	[15]
Zn	1.20×10^{1}	2023	[16]
Ni	3.60×10^{0}	2023	[17]
Epoxy resin	3.60×10^{0}	2022	[18]
PVC	5.10×10^{1}	2022	[10]
Cr	4.10×10^{1}	2021	[19]
Co	2.00×10^{-1}	2023	[20]
Si	3.80×10^{0}	2023	[21]

*1.92×10^{3} million m^3 assuming 555 kg/m^3, **forecast from 2016

Table S2: Steel intensities of renewable energy systems. Intensity includes additional steel needed to replace Al in PV mounting systems.

Technology	**Steel per capacity [kg/MW]**
photovoltaics, open-ground	5.50×10^{4}
photovoltaics, slanted-roof	2.98×10^{4}
wind energy, offshore	9.48×10^{4}
wind energy, onshore	1.52×10^{5}

S3 Steel production cost

Secondary steel production is competitive with primary steel production (see Fig. S2) and can even be slightly cheaper (-0.3 %, -5.1 %, and -6.3 % less production cost for reinforcing, low-alloyed, and chromium steel respectively on plant average) [22].

S4 Capacity potential of steel

Table S2 shows the steel intensities of solar photovoltaic (PV) and wind energy systems (accounting for steel used to substitute Al). Table S3 shows the maximum energy system capacity that can be built with the steel embedded in the current fossil infrastructure. The fossil steel stock is sufficient to build 24.44 and 45.12 TW_p of open-ground and slanted-roof PV, and 14.18 and 8.84 TW_p of offshore and onshore wind capacity respectively. This is 2.5 to 4.7 times the PV, and 1.7 to 2.8 times the wind capacity projected for 2050 in the SSP2-NPi scenario.

S5 Steel use in photovoltaic systems

Aluminum (Al) is used in PV mounting systems to connect the module to a surface (e. g., roof, ground). We test the environmental effect of using steel instead of Al for mounting the module. To estimate the

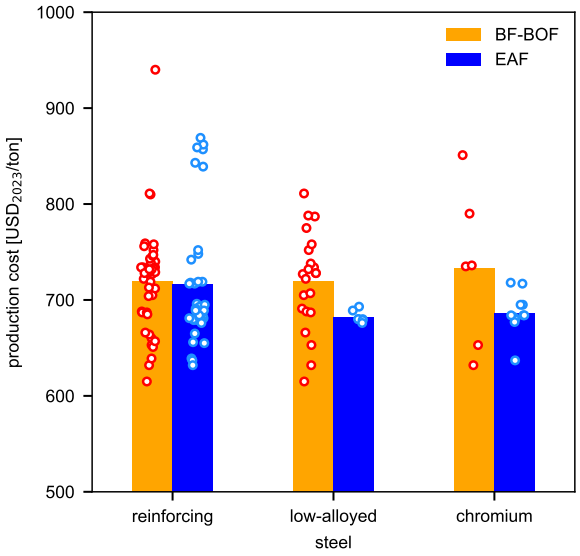

Figure S2: **Steel production cost for blast furnace basic oxygen furnace route (BF-BOF) and electric arc furnace route (EAF) in the year 2021**. The production cost of 125 individual steel plants in 63 countries (red and blue dots). Bar shows the plant average production cost. Data taken from [22].

Table S3: Capacity of solar and wind energy systems that can be built with steel in current fossil infrastructure (median steel stock) and capacity in 2050 according to the SSP2-NPi scenario. Intervals cover the steel intensities of open-ground and slanted for solar PV and on- and offshore for wind energy respectively.

	Capacity [TW_p]	
Technology	**Steel potential**	**Installed SSP2-NPi 2050**
Solar PV	[2.44, 4.51]$\times 10^1$	0.96$\times 10^1$
Wind	[0.88, 1.42]$\times 10^1$	0.51$\times 10^1$

steel needed for this purpose we assume two L-shaped steel profiles with 0.03 m height and width, a thickness of 0.003 m, and a length of 1.08 m to mount a module with the dimensions of 1 m$\times$1.85 m. With a steel density of 7,860 kg/m^3, this yields 1.53 kg steel per m^2 or 0.54 kg steel per substituted kg Al (Al intensity taken from ecoinvent v3.9.1 for slanted-roof PV; 2.84 kg Al per m^2). For open-ground PV systems, we substitute Al with the same factor of 0.54 kg steel per kg Al.

S6 Carbon footprints of green hydrogen and methanol

We assess the cascading effect of greener production of renewable energy systems when using repurposed steel from fossil infrastructure. As ogPV benefits the most from using secondary steel instead of Al in mounting systems, we test the reduction potential in chemical production with open-ground PV in the case of Spain in the year 2025 following an SSP2-NPi scenario. The default case is a mix of both primary steel and aluminum in the open-ground PV, whereas both are substituted with recycled steel from fossil infrastructure in the recycled steel case (ogPVr).

We test different electrolyzers and pressure levels of hydrogen. The carbon footprint of hydrogen is reduced by 26 % to 30 % when supplying ogPVr electricity, achieving footprints below 1 kg $CO_{2,eq}$/kg (see Fig. S3). This is lower than values found in the literature [23], however, we use more up-to-date inventories for PV systems, more efficient single-Si instead of multi-Si cells, and lower impact mounting systems.

We test further processing of green hydrogen into green methanol production by also testing the supply

of ogPVr electricity in direct air capture CO_2 production. The combined effect yields a 6 % reduction in the carbon footprint of green methanol compared to using default open-ground PV systems. Although this case study is not spatially or temporally representative of global green hydrogen production, it shows the potential of substituting for steel in renewable energy systems to reduce the footprints of energy-intensive chemicals.

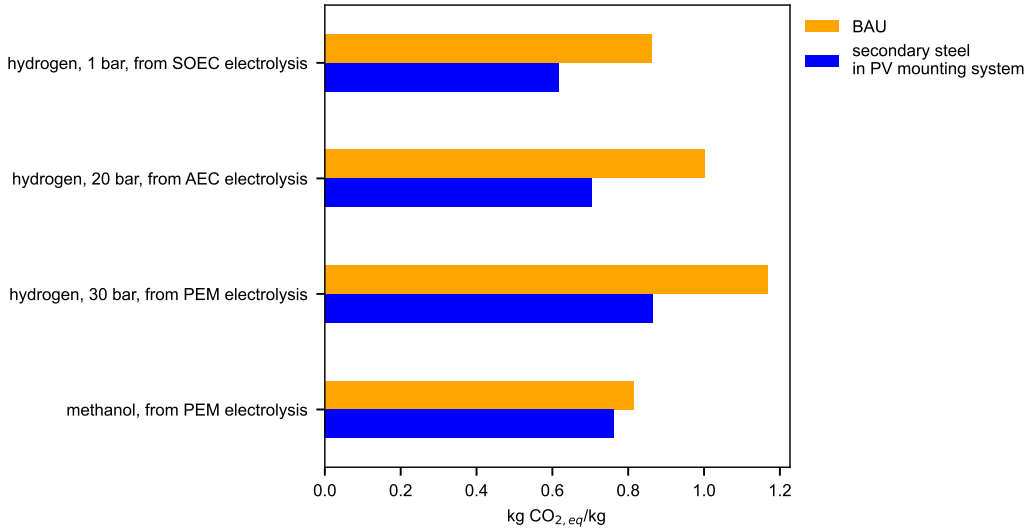

Figure S3: **The carbon footprint of green hydrogen and green methanol production in Spain.** Business-as-usual (BAU) scenario reflects raw material production (hydrogen electrolysis and direct air capture of CO_2) electricity supply from PV with current Aluminum mounting systems (orange bar). BAU scenario is compared to carbon footprint of green hydrogen and methanol production using recycled steel in PV mounting systems (blue bar). In both scenarios, the electricity source is open-ground PV following SSP2-NPi in the year 2025. SOEC=solid oxide electrolyzer, AEC=alkaline electrolyzer, PEM=proton exchange membrane electrolyzer.

S7 Value of steel scrap in fossil infrastructure

For private fossil companies, the economic value of steel scrap could be an incentive for decommissioning infrastructure. Between February 2019 and February 2020, the ferrous scrap selling prices ranged from 257 to 479 USD_{2023} between regions [24]. For a back-of-the-envelope calculation, we assume a selling price of 350 USD_{2023} per ton and a potentially recyclable stock of 1.35 Gt steel scrap in current fossil infrastructure, yielding a total of 472 billion USD_{2023} worth of ferrous scrap in current global fossil infrastructure.

S8 Limitations and robustness of results

- We likely underestimate the soon-to-be-obsolete fossil stock, as we excluded oil refineries or internal combustion engine cars, as they could be refurbished into bio-refineries and electric cars. Stocks of steel are in the range of other estimates (1.35 [0.84–2.26] Gt) is in reasonable agreement with literature values (0.5–2.0 Gt) [25, 26]).
- We excluded biomass utilization in steel-making, which might reduce climate impacts of primary steel production, albeit at the trade-off with land and water use.
- Recycling is one of several circular strategies that could be applied to obsolete infrastructures. Other strategies, such as reusing pipelines in district heating networks or reusing power plant sites for grid storage infrastructure could potentially avoid more costs and impacts or bring other advantages

due to narrower cycles. Future research can compare different circular strategies to find potential synergies or trade-offs.

- We exclude dynamic implications of potentially accelerating the energy transitions by avoiding material supply bottlenecks for building renewable energy infrastructure (e. g., Al shortage). Especially in times of geopolitical tensions and the concurrent need to accelerate climate action, materials may not be available in the needed quantity and quality. Digesting fossil infrastructure may serve as a strategy to mitigate such supply shortages. The cumulative environmental benefit may thus be larger than the direct impact savings calculated in this study.
- The general conclusions remain valid under pessimistic assumptions for scrap quality and slag composition and possible trade-offs with water use and ionizing radiation can be tackled by optimizing the electricity supply. Maintaining a high scrap quality is important, which can be achieved if waste flows from fossil infrastructure stay unmixed, reducing the need for dilution.
- Leakage of hexavalent chromium (Cr^{6+}) from slags, which are produced in EAFs when chromium steel is present in the scrap, can undermine the benefits of steel recycling. Several EAF waste treatments exist that can reduce the leaching of toxic Cr^{6+} from slag [27–32] and dust [33, 34], but it is unclear how far these treatments are industrial practice. Adopting such slag and dust treatments is important to lower impact on human health.

S9 Material intensities of fossil infrastructure and their uncertainty

S9.1 Material intensities

Figure S4 shows material intensities for fossil infrastructure assessed based on ecoinvent v3.9.1 [35]. Detailed uncertainty values can be found in the data repository of this study. The fossil infrastructure inventory values taken from ecoinvent v3.9.1 cannot be publicized due licensing reasons but can be made available upon request to interested readers with ecoinvent license.

S9.2 Uncertainties

Multiple sources of uncertainties exist regarding material stocks in fossil infrastructure. 1) Uncertainties arise from the geographical and temporal variability of infrastructure, which is modeled with log-normal distributions for each material intensity in ecoinvent. The standard deviation for each material intensity can be accessed in the data repository. 2) Some material intensities, such as wood and concrete, are reported as volume and require translation to mass using densities. The density uncertainties for these materials are shown in Table S4. 3) Fossil infrastructure is classified differently in ecoinvent and in Global Energy Monitor (GEM) databases. This generates linking uncertainty in selecting the representative material intensity for some infrastructure types. We model these uncertainties by a uniform distribution covering the range between minimum and maximum possible material intensities arising from linking choices (see data repository for values). For example, a power plant with 350 MW capacity can either be assigned material intensities of a 100 MW or 500 MW power plant. In the case of this linking choice, we adopt a threshold (e. g., 300 MW) to assign the infrastructure to the more representative infrastructure class. Threshold values are shown in Table S5.

Furthermore, some infrastructure classes in GEM databases [36] are not present in ecoinvent, such as combined underground and surface coal mines (open pit) as well as refuse coal mines (surface coal wastes at coal mines). We model the material intensities of combined underground and surface coal mine as the mean of an underground and surface coal mine, and the refuse coal mine as an open pit mine.

The material intensity of oil and gas extraction infrastructure is sensitive to borehole length. As the GEM database does not indicate the borehole length of individual wells, we take 3,000 m being the mean of 17,540 oil wells in the Bakken Formation [37] and account for possible other borehole lengths in the linking uncertainty (assuming a minimum of 1,000 m and a maximum of 5,000 m borehole length, being the range indicated in [37]).

We propagate all uncertainty by running a Monte Carlo simulation ($n = 500$), generating a distribution of possible material stocks for each infrastructure.

Table S4: Volumetric density parameters and their uncertainty for selected materials.

Material	**Uncertainty type**	**Min [kg/m^3]**	**Mode [kg/m^3]**	**Max [kg/m^3]**	**Sigma**	**Remark**
plywood	uniform	4.00×10^2	5.50×10^2	7.00×10^2		assumed
sawnwood, hardwood, raw, dried (u=20%)	uniform	3.50×10^2	5.60×10^2	7.70×10^2		assumed
concrete, normal strength	normal		2.35×10^3		6.96×10^1	ecoinvent v3.9.1
unreinforced concrete, 15MPa	normal		2.35×10^3		6.96×10^1	ecoinvent v3.9.1
Wood*	uniform	3.50×10^2	5.60×10^2	7.70×10^2		assumed
Concrete*	normal		2.35×10^3		6.96×10^1	ecoinvent v3.9.1

*aggregated material category

Table S5: Threshold values for linking infrastructure classes.

Infrastructure	**Threshold**	**Interval**	**Unit**	**Variable**
hard coal power plant	3.00×10^2	[1.00, 5.00]$\times10^2$	MW	capacity
gas power plant	2.00×10^2	[1.00, 3.00]$\times10^2$	MW	capacity
pipeline, natural gas, long distance, onshore	0.95×10^6	[0.8, 1.1]$\times10^6$	norm m^3/h	throughput
pipeline, natural gas, long distance, onshore	1.085*	[0.950, 1.219]	m	diameter

*if throughput data missing

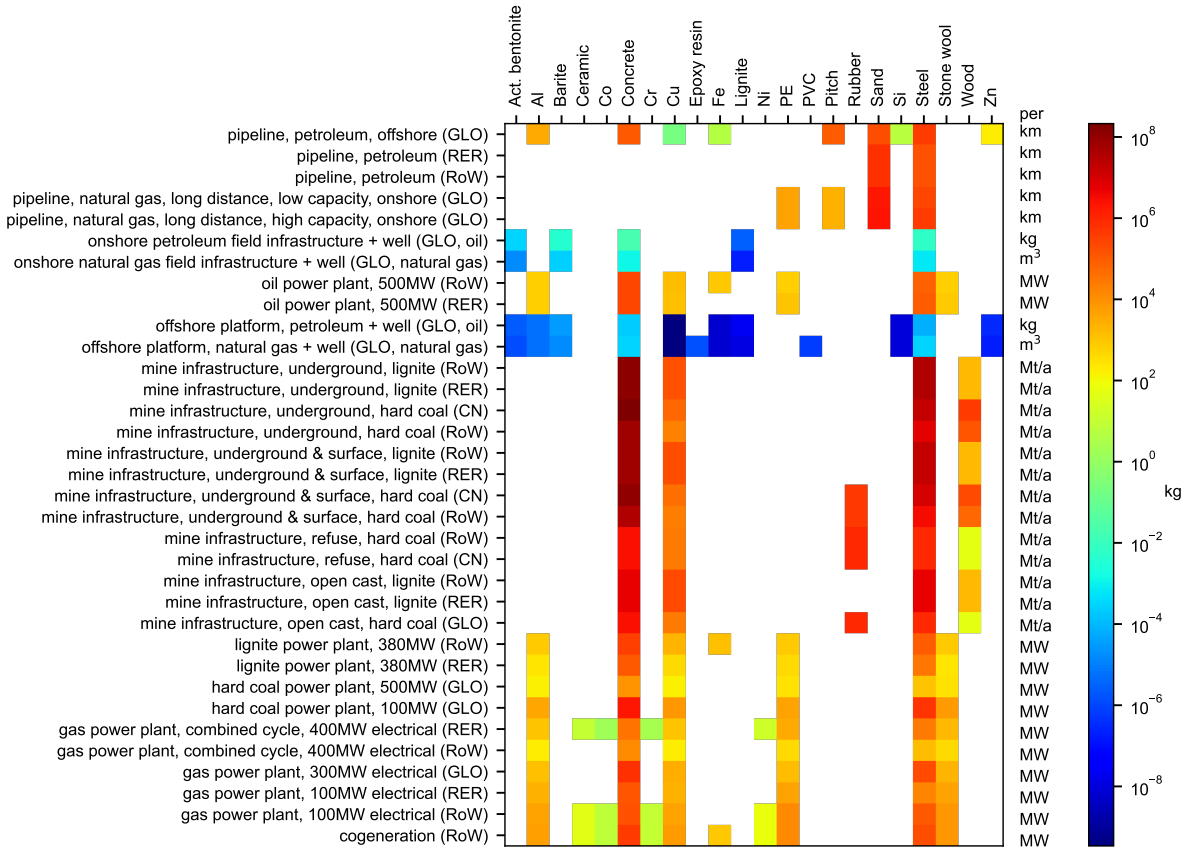

Figure S4: **Normalized material intensities of fossil infrastructure.** Oil and gas rig material intensities are shown normalized to kg and cubic meters of oil and gas extracted respectively, coal mine intensities are normalized to Mt/a coal extraction capacity, power plant material intensities are normalized to power capacity, and pipelines material intensities per kilometer length. Brackets indicate geographical region (GLO=global, RER=Europe, RoW=Rest of World, CN=China) and fuel type in case of oil and gas rigs. Abbreviations of materials are Cr for Chromium, PE for polyethylene, Ni for Nickel, Co for Cobalt, PVC for polyvinyl chloride, Si for Silicon, Zn for Zinc, Cu for Copper, Fe for Iron, and Al for Aluminum.

S10 Steel life cycle assessment

S10.1 Goal, scope, and system boundaries

The functional unit of the life cycle assessment is the production of the steel equivalent to the amount currently stored in fossil infrastructure—either by the secondary (electric arc furnace) or primary route (blast furnace and basic oxygen furnace). The geographical scope is global and the temporal scope is 2025 to 2050 in five-year intervals.

System boundaries for the life cycle assessment foreground system modeled are shown for the secondary and primary production routes in Figures S5 and S6 respectively. We adapt gate-to-gate production inventories from [1] (based on [38]) and expand to cradle-to-gate boundaries for scrap supply from fossil infrastructure for the EAF production route. All flows outside of system boundaries are accounted for in the background systems.

The life cycle inventories are available in the data repository associated with this article.

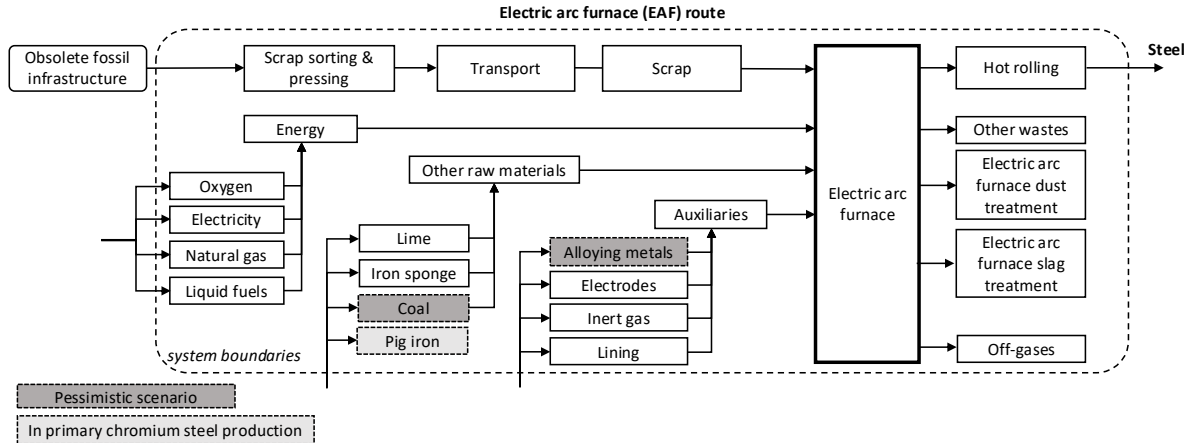

Figure S5: **System boundaries for steel-making via electric arc furnaces.** The foreground system of secondary steel production includes energy, raw material, and auxiliary inputs as well as hot rolling, off-gases, and process waste treatments. Coal and alloying metal flows are set to zero in the optimistic scenario. Inventory adapted from [1].

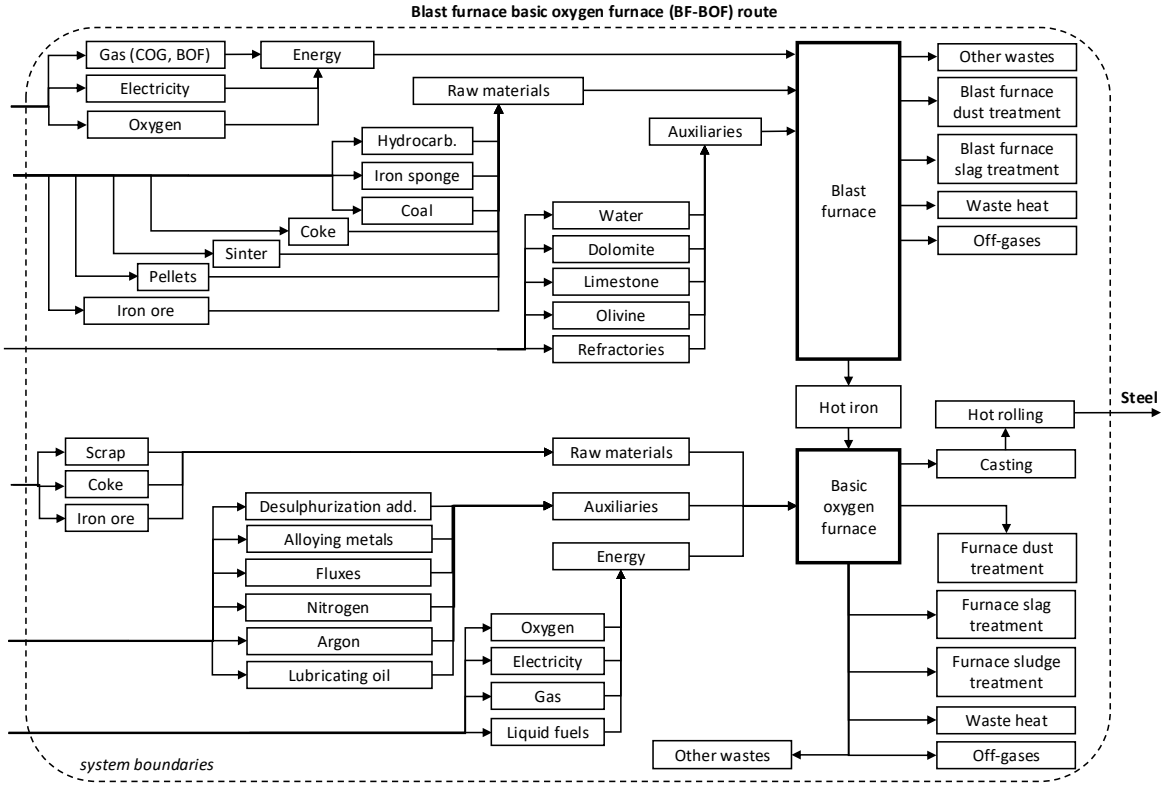

Figure S6: **System boundaries for iron-making via blast furnace and steel-making via basic oxygen furnace.** The foreground system of primary steel production includes energy, raw material, and auxiliary inputs as well as casting, hot rolling, off-gas emissions, and process waste treatments. Inventory adapted from [1]. COG=cogeneration, BOF=basic oxygen furnace.

S10.2 Scrap transport estimation

We estimate a globally representative scrap transport distance from fossil infrastructure to recycling plants by weighing distances within countries and between countries. To yield a representative transport distance within a country, the distance of each fossil infrastructure to the closest recycling plant (assuming it to be the most economical option) is calculated and weighed by the mass share of the total country steel waste stock in fossil infrastructure (see Eq. 1). The representative country distances are then weighted by the share of country stocks of scrap (Eq. 2).

$$D_c = f_r \frac{1}{s_{c,total}} \sum_{n \in N_c} d_n \cdot s_n \quad \forall c \in C \tag{1}$$

$$D_{GLO} = \frac{1}{s_{total}} \sum_{c \in C} D_c \cdot s_{c,total} \tag{2}$$

D_c is the representative scrap transport distance in country c (an element of all assessed countries C), n is a fossil infrastructure in the set of all the country's fossil infrastructure N_c, d_n is the distance of n to the closest recycling plant (the straight line between two points on a globe), and s_n is the steel scrap stock in n. The route factor f_r corrects for the fact that real transport distances are longer than the ideal distances (straight line) and is assumed to be 1.5. The total scrap stock in country c is $s_{c,total}$, and s_{total} is the global total scrap stock in fossil infrastructure. D_{GLO} is the global representative scrap transport distance, which is 481 m if the scrap is transported to the closest recycling plant. This is in good agreement with the 537 km that ecoinvent v3.9.1 assumes for sorted and pressed iron scrap in Rest of World. The transport mode split is the scrap stock weighted average of countries (assuming global mode split, in those instances where country-level data is missing).

S10.3 Steel production efficiencies

Different steel production efficiencies are assumed for investigated scenarios. Figure S7 shows process inputs (e. g., coal, natural gas, electricity, ferromanganese), carbon emissions, and carbon capture relative to process flows in SSP1-NDC. Efficiency gains target the blast furnace, basic oxygen furnace (primary) route, and the electric arc furnace (secondary) route. Values are taken from Premise [1].

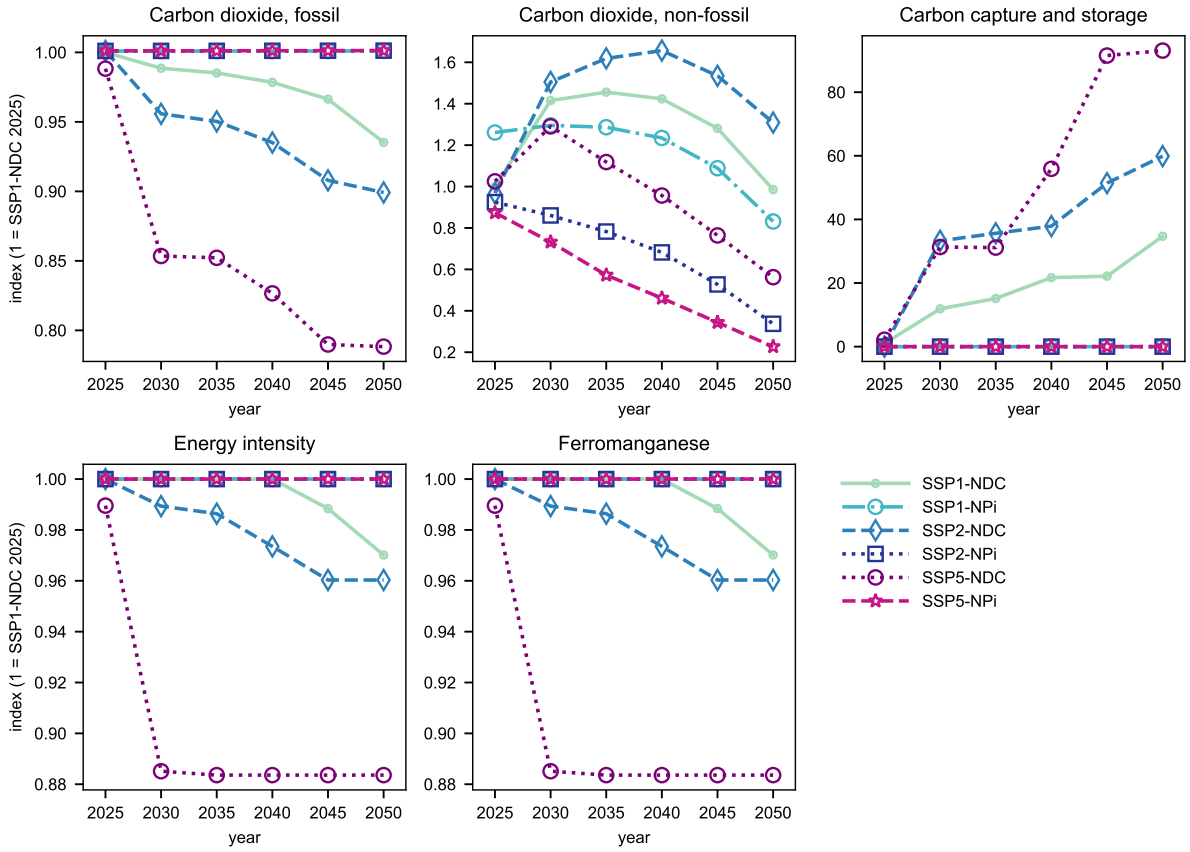

Figure S7: **Process efficiencies**. Efficiencies of process inputs and emissions in primary and secondary steel production depending on the scenario. All input amounts are normalized to SSP1-NDC 2025. Efficiencies are taken from Premise [1].

S10.4 Inventory adjustments for electric arc furnace hexavalent chromium content in slag and dust

Cr^{6+} creates adverse health effects in humans and other organisms [39,40] and can leak from electric arc furnace slag and dust into the environment. The content of Cr^{6+} in slag and dust can vary significantly, which is why we modify the standard ecoinvent inventory to capture the range of potentially leaking Cr^{6+} by selecting low and high values found in literature for the optimistic and pessimistic scenarios respectively.

We also adjust Cr^{6+} release in electric arc furnace slag treatment in ecoinvent, as ecoinvent likely overestimates Cr^{6+} leaching. Measurements of Cr^{6+} content in electric arc furnace slag from 58 steel mills [41] yield a mean of 1.2 mg Cr^{6+}/kg slag. We take the 2.5 percentile assuming a log-normal distribution as the optimistic value (0.14 mg Cr^{6+}/kg slag) and the 97.5 percentile as the pessimistic value (67.17 mg Cr^{6+}/kg slag)—which is significantly lower than 7.05×10^{3} mg Cr^{6+}/kg, assumed on ecoinvent. We assume that half the Cr^{6+} is emitted to groundwater and half to surface water.

The chemical composition of electric arc furnace dust can vary, depending on the chemical composition of steel scrap and operating conditions [42]. Due to missing representative literature data on Cr^{6+} release from dust, we adopt the uncertainty range indicated in *treatment of electric arc furnace dust, residual material landfill* (RoW) taken from ecoinvent v3.9.1. As an optimistic scenario, we assume the 2.5 percentile of Cr^{6+} release, yielding 2.07×10^{-4} kg and 5.03×10^{-5} kg per kg dust to groundwater and surface water respectively. As a pessimistic scenario, we take the 97.5 percentile of the emission uncertainty, yielding 3.94×10^{-3} kg and 1.46×10^{-3} Cr^{6+} kg per kg dust to groundwater and surface water respectively.

S11 Life cycle impact indicators

We translate midpoint indicators—usually emissions—into damage to human health and ecosystems as well as pressures on natural resources (endpoint indicators) according to the ReCiPe Framework 2016 v1.1 ([43]; see Fig. S8, S9, and S10). Human health-related environmental impacts are converted to human health impacts in units of Disability Adjusted Life Years (DALYs), ecosystem-related midpoint indicators are converted into ecosystem damage in units of species years lost, and fossil and mineral extraction into surplus cost potential in units of US dollars.

All life cycle impact assessment methods used to calculate midpoint indicators and their respective characterization factors are available in the data repository.

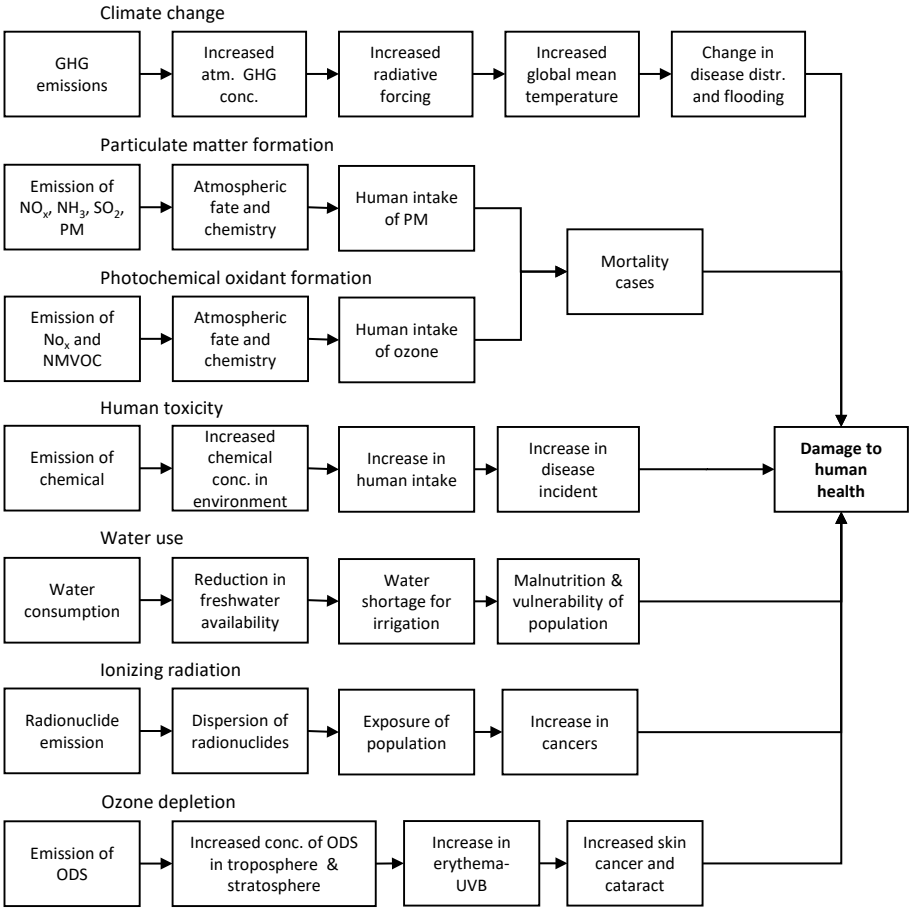

Figure S8: **Cause-and-effect chain of midpoint indicators to human health impact.** Figure based on ref. [44]. GHG: Greenhouse gas emissions, PM: Particular matter, NMVOC: Non-methane volatile organic compounds, ODS: Ozone depleting substances, UVB: Ultraviolet B radiation.

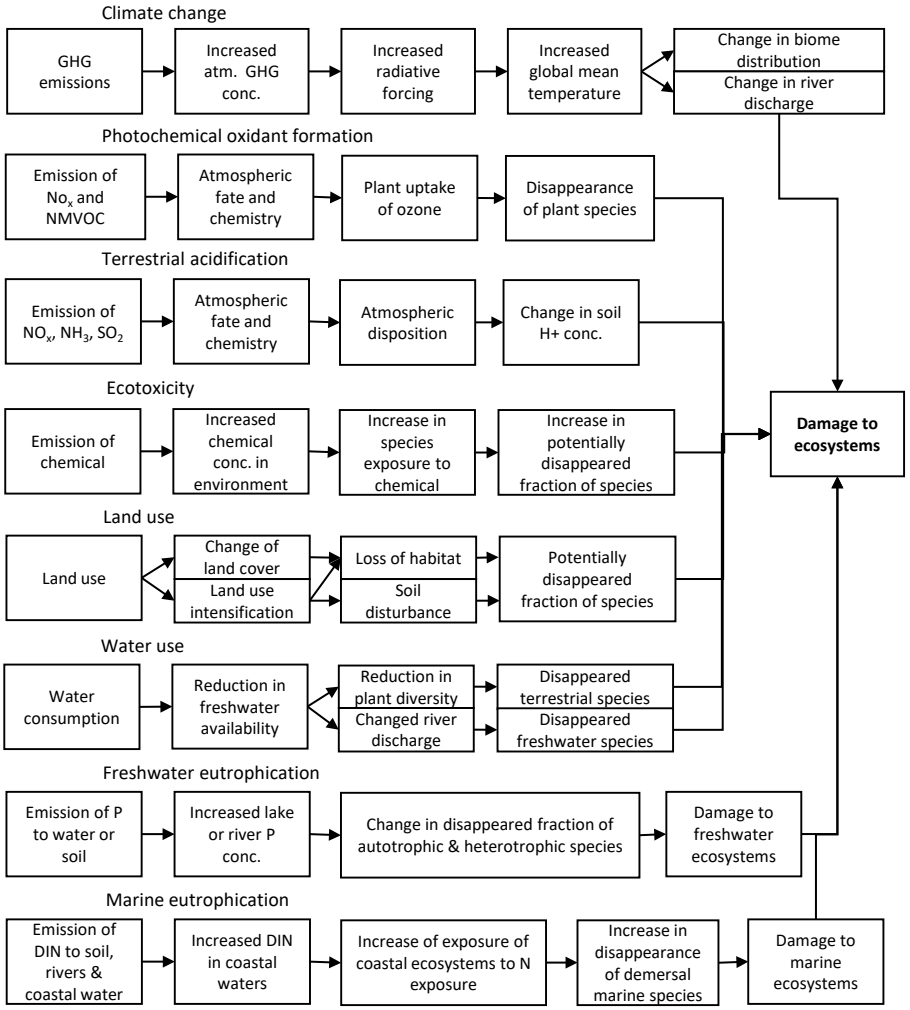

Figure S9: **Cause-and-effect chain of midpoint indicators to ecosystem damage.** Figure based on ref. [44]. GHG: Greenhouse gas emissions, NMVOC: Non-methane volatile organic compounds, DIN: Dissolved inorganic nitrogen.

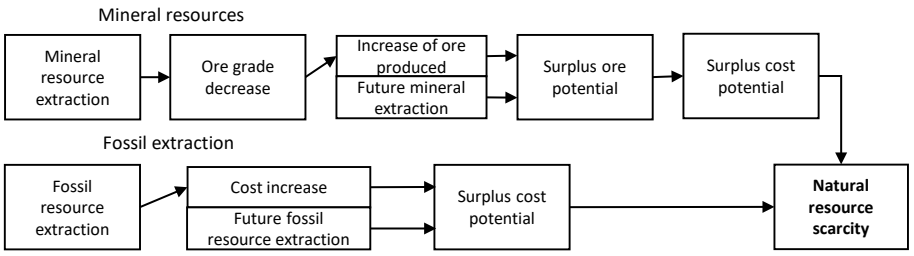

Figure S10: **Cause-and-effect chain of midpoint indicators to natural resource scarcity.** Figure based on ref. [44]. Natural resource scarcity is driven by mineral and fossil resource extraction.

References

[1] Sacchi, R. *et al.* Prospective environmental impact assement (premise): A streamlined approach to producing databases for prospective life cycle assessment using integrated assessment models. *Renewable and Sustainable Energy Reviews* **160**, 112311 (2022). http://dx.doi.org/10.1016/j.rser.2022.112311.

[2] *Paris agreement*. (United Nations Framework Convention on Climate Change, 2015). Retrieved at https://unfccc.int/process-and-meetings/the-paris-agreement/the-paris-agreement.

[3] *2100 warming projections: Emissions and expected warming based on pledges and current policies. November 2024*. (Climate Analytics and NewClimate Institute, 2024). https://climateactiontracker.org/global/temperatures/.

[4] Monteiro, P. J. M., Miller, S. A. & Horvath, A. Towards sustainable concrete. *Nature Materials* **16**, 698–699 (2017).

[5] *Sand and sustainability: 10 strategic recommendations to avert a crisis*. (United Nations Environment Programme, 2022).

[6] *Mineral Commodity Summaries 2024: Iron and Steel*. (U.S. Geological Survey, 2024). https://pubs.usgs.gov/periodicals/mcs2024/mcs2024-iron-steel.pdf.

[7] *Global forest products facts and figures 2023*. (Food and Agriculture Organisation, 2024). http://dx.doi.org/10.4060/cd3650en.

[8] *Mineral Commodity Summaries 2022: Clays*. (U.S. Geological Survey, 2022). https://pubs.usgs.gov/periodicals/mcs2022/mcs2022-clays.pdf.

[9] *Mineral Commodity Summaries 2024: Barite*. (U.S. Geological Survey, 2024). https://pubs.usgs.gov/periodicals/mcs2024/mcs2024-barite.pdf.

[10] *Plastics – the fast Facts 2023*. (Plastics Europe, 2023). https://plasticseurope.org/de/wp-content/uploads/sites/3/2023/11/PlasticsthefastFacts2023_printing.pdf.

[11] *Mineral Commodity Summaries 2024: Copper*. (U.S. Geological Survey, 2024). https://pubs.usgs.gov/periodicals/mcs2024/mcs2024-copper.pdf.

[12] *Market volume of the insulation material market worldwide in 2016, with a forecast for 2021, by material*. (Statista, 2016). Last accessed December 29th 2024 at https://www.statista.com/statistics/911536/insulation-material-market-volume-worldwide-by-material/.

[13] *Mineral Commodity Summaries 2022: Aluminum*. (U.S. Geological Survey, 2022). https://pubs.usgs.gov/periodicals/mcs2022/mcs2022-aluminum.pdf.

[14] *Consumption of natural and synthetic rubber worldwide from 1990 to H1 2024*. (Statista, 2024). Last accessed December 29th 2024 at https://www.statista.com/statistics/911536/insulation-material-market-volume-worldwide-by-material/.

[15] *Coal Information*. (International Energy Agency, 2021). https://www.iea.org/reports/coal-information-overview/production.

[16] *Mineral Commodity Summaries 2024: Zinc*. (U.S. Geological Survey, 2024). https://pubs.usgs.gov/periodicals/mcs2024/mcs2024-zinc.pdf.

[17] *Mineral Commodity Summaries 2024: Nickel*. (U.S. Geological Survey, 2024). https://pubs.usgs.gov/periodicals/mcs2024/mcs2024-nickel.pdf.

[18] *Epoxy Resin Market Size, Growth, and Forecast, 2030*. (Statista, 2024). Last accessed March 25th 2025 at https://www.chemanalyst.com/industry-report/epoxy-resin-market-597#:~:text=The%20global%20Epoxy%20Resin%20market,other%20monomers%20containing%20hydroxyl%20group..

[19] *Mineral Commodity Summaries 2024: Chromium*. (U.S. Geological Survey, 2024). https://pubs.usgs.gov/periodicals/mcs2022/mcs2022-chromium.pdf.

[20] *Statistical Review of World Energy (2024). 73rd Edition*. (Energy Institute, 2024). https://www.energyinst.org/statistical-review.

[21] *Mineral Commodity Summaries 2024: Silicon*. (U.S. Geological Survey, 2024). https://pubs.usgs.gov/periodicals/mcs2024/mcs2024-silicon.pdf.

[22] *Global steel cost tracker*. (TransitionZero, 2022). Data retrieved from https://www.transitionzero.org/products/global-steel-cost-tracker.

[23] Weidner, T., Tulus, V. & Guillén-Gosálbez, G. Environmental sustainability assessment of large-scale hydrogen production using prospective life cycle analysis. *International Journal of Hydrogen Energy* **48**, 8310–8327 (2023). http://dx.doi.org/10.1016/j.ijhydene.2022.11.044.

[24] *Ferrous Scrap Prices | Current and Forecast*. (Intratec, 2025). Last accessed February 28th 2025 at https://www.intratec.us/chemical-markets/ferrous-scrap-price.

[25] Le Boulzec, H. *et al.* Dynamic modeling of global fossil fuel infrastructure and materials needs: Overcoming a lack of available data. *Applied Energy* **326**, 119871 (2022).

[26] Deetman, S., de Boer, H. S., Van Engelenburg, M., van der Voet, E. & van Vuuren, D. P. Projected material requirements for the global electricity infrastructure–generation, transmission and storage. *Resources, Conservation and Recycling* **164**, 105200 (2021).

[27] Tae, S. & Morita, K. Immobilization of Cr (VI) in stainless steel slag and Cd, As, and Pb in wastewater using blast furnace slag via a hydrothermal treatment. *Metals and Materials International* **23**, 576–581 (2017).

[28] Lin, Y., Yan, B., Fabritius, T. & Shu, Q. Immobilization of chromium in stainless steel slag using low zinc electric arc furnace dusts. *Metallurgical and Materials Transactions B* **51**, 763–775 (2020).

[29] Strandkvist, I. *et al.* Minimizing chromium leaching from low-alloy electric arc furnace (EAF) slag by adjusting the basicity and cooling rate to control brownmillerite formation. *Applied Sciences* **10**, 35 (2019). http://dx.doi.org/10.3390/app10010035.

[30] Spanka, M., Mansfeldt, T. & Bialucha, R. Influence of Natural and Accelerated Carbonation of Steel Slags on Their Leaching Behavior. *Steel Research International* **87**, 798–810 (2016). http://dx.doi.org/10.1002/srin.201500370.

[31] Mombelli, D., Gruttadauria, A. & Mapelli, C. The Influence of Slag Tapping Method on the Efficiency of Stabilization Treatment of Electric Arc Furnace Carbon Steel Slag (EAF-C). *Minerals* **9**, 706 (2019). http://dx.doi.org/10.3390/min9110706.

[32] Cao, S., Sohn, I. & Wang, Z. Selective stabilization of chromium and sustainable treatment of stainless steel slags. *Journal of Environmental Chemical Engineering* **12**, 113516 (2024). http://dx.doi.org/10.1016/j.jece.2024.113516.

[33] Wang, J. *et al.* Pyrometallurgical recovery of zinc and valuable metals from electric arc furnace dust–a review. *Journal of Cleaner Production* **298**, 126788 (2021).

[34] Xu, J. *et al.* Valuable recovery technology and resource utilization of chromium-containing metallurgical dust and slag: a review. *Metals* **13**, 1768 (2023).

[35] Wernet, G. *et al.* The ecoinvent database version 3 (part i): overview and methodology. *The International Journal of Life Cycle Assessment* **21**, 1218–1230 (2016). www.doi.org/10.1007/s11367-016-1087-8.

[36] *Global coal mine tracker, July 2022 release*. (Global Energy Monitor, 2022). Data retrieved from https://globalenergymonitor.org/projects/global-coal-mine-tracker/.

[37] Parish, E. S. *et al.* Comparing scales of environmental effects from gasoline and ethanol production. *Environmental management* **51**, 307–338 (2013).

[38] *Best Available Techniques (BAT) Reference Document for Iron and Steel Production*. (Joint Research Centre, 2013). www.doi.org/10.2791/97469.

[39] Welling, R. *et al.* Chromium VI and stomach cancer: a meta-analysis of the current epidemiological evidence. *Occupational and Environmental Medicine* **72**, 151–159 (2014).

[40] Prasad, S. *et al.* Chromium contamination and effect on environmental health and its remediation: A sustainable approaches. *Journal of Environmental Management* **285**, 112174 (2021).

[41] Proctor, D. M. *et al.* Physical and chemical characteristics of blast furnace, basic oxygen furnace, and electric arc furnace steel industry slags. *Environmental Science & Technology* **34**, 1576–1582 (2000).

[42] Omran, M. & Fabritius, T. Effect of steelmaking dust characteristics on suitable recycling process determining: Ferrochrome converter (CRC) and electric arc furnace (EAF) dusts. *Powder Technology* **308**, 47–60 (2017).

[43] Huijbregts, M. *et al.* Recipe2016 - a harmonised life cycle impact assessment method at midpoint and endpoint level. *International Journal of Life Cycle Assessment* **22**, 138–147 (2017). www.doi.org/10.1007/s11367-016-1246-y.

[44] *ReCiPe 2016 v1.1 A harmonized life cycle impact assessment method at midpoint and endpoint level. Report I: Characterization*. (National Institute for Public Health and the Environment, 2017). https://www.rivm.nl/documenten/recipe2016v11.

[45] *Global energy transformation: A roadmap to 2050*. (International Renewable Energy Agency, 2019).

[46] Byers, E., *et al.* AR6 scenarios database In *Climate Change 2022: Mitigation of Climate Change (1.1). Integrated Assessment Modeling Consortium & International Institute for Applied Systems Analysis*. (2022). https://doi.org/10.5281/zenodo.5886911.